Three-Dimensional Structure and Motion of Twist Grain Boundaries in Block Copolymer Melts

Andriy V. Kyrylyuk*,† and Johannes G. E. M. (Hans) Fraaije‡

Laboratory of Macromolecular Chemistry and Nanoscience, Eindhoven University of Technology and Dutch Polymer Institute (DPI), P.O. Box 513, 5600 MB Eindhoven, The Netherlands, and Soft Matter Chemistry Group, Leiden Institute of Chemistry, Leiden University, P.O. Box 9502, 2300 RA Leiden, The Netherlands

Received May 3, 2005; Revised Manuscript Received June 28, 2005

ABSTRACT: The three-dimensional structure and motion of twist grain boundaries in lamella forming diblock copolymer melts in the presence of an external electric field were studied by means of computer simulations. The method used is a mean-field dynamic density functional theory with electrostatic interactions incorporated into the model. The observed twist grain boundary structure consists of a doubly periodic array of saddle surfaces, similar to Scherk's first surface. We found that the twist grain boundary interface remains unbroken, and the grain boundary structure keeps its profile constant during twist grain boundary motion. This suggests that twist grain boundaries move via a mechanism in which only diffusion parallel to the interfaces is necessary. The twist grain boundary motion is a specific case of a more general mechanism of mesophase reorientation by defect movement. The width of a twist grain boundary is found to be about the lamellar period for all the observed twist angles, corroborating the fact that the twist grain boundary interface basically is built from one layer of diblock copolymer chains. The existence of twisted lamellae grains causes a large domain contribution to the stress tensor arising from the composition inhomogeneities. The results of our simulations demonstrate that the motion of a twist grain boundary is not affected by the electric field, which differs from the movement of a grain boundary under shear flow. Such a distinction in behavior originates from the difference in symmetry of shear and electric field. In contrast with microphase-separated block copolymer in an electric field, in the sheared systems, defects in microstructure are convected by the flow field. Because of the uniaxial symmetry of a system with respect to the applied electric field, which facilitates the creation of twist grain boundaries and suppresses tilt grain boundaries, an electric field is a perfect candidate to investigate twist grain boundary motion.

I. Introduction

Block copolymers, in which two or more chemically different subchains form a single macromolecule, are a fascinating class of soft materials with unique structural, mechanical, and electrical properties.[1−3] Below an order-to-disorder transition temperature, block copolymers are able to self-assemble into a variety of ordered structures with domain sizes in the nanometer range. For diblock copolymers, these equilibrium structures range from lamellar, hexagonal-packed cylinder, and body-centered-cubic sphere phases to complex cubic bicontinuous (gyroid) morphologies. The phase behavior of diblock copolymer melts can be controlled by varying the chemical composition of the diblock copolymer and the segregation between blocks (via temperature or molecular weight) or by applying external fields.

Self-assembling block copolymer systems that can order into periodic arrays of nanoscopic structures have potential use in applications from optics to microelectronics.[4,5] The use of block copolymers in photonic and electronic devices requires the production of single crystals. However, achieving uniform orientation in these materials is not trivial. Without external fields, a macroscopic size sample usually exhibits polycrystalline structure consisting of many block copolymer domains (grains). The ordering of the domains is high locally, but globally the orientation of the domains, on average, is random. It has been demonstrated that the desired long-range microdomain orientation can be achieved by the application of an external electric field,[6−26] shear field,[27−36] or temperature gradient.[37,38]

The structure of the boundary regions between grains influences mechanical, electrical, and transport properties of block copolymers to a great extent. The three-dimensional (3D) continuity of each microphase at a grain boundary, which is maintained across the boundary, plays an important role in determining the material properties of block copolymers.[39−41] The presence of grain boundaries as well as other topological defects destroys the global long-range orientation of the block copolymer morphology, which in turn changes the properties of the system. Grain boundaries and other topological defects in a microstructure are nonequilibrium, metastable morphologies, which structure and especially kinetics are not yet well-understood. The motion of grain boundaries plays an important role in the global alignment of microdomains under an electric field or shear. The mechanisms of grain boundary motion can be different depending on the type of a grain boundary and symmetry of the externally applied field.

Much experimental and theoretical effort has been made to study grain boundary structures and their motion.[29−32,34−36,39−54] Grain boundaries in 3D space have five degrees of twist−tilt freedom.[42,43] Lamellar block copolymers, exhibiting one-dimensional symmetry, have grain boundaries for which only two of those degrees are important. Consequently, the grain boundaries in lamella forming block copolymers can be divided

† Eindhoven University of Technology and Dutch Polymer Institute.
‡ Leiden University.

10.1021/ma0509356 CCC: $30.25
Published on Web 08/30/2005

into two independent ones: the tilt (kink) grain boundary and the twist grain boundary (TGB). In the tilt grain boundary, the normals to the lamellae of two neighboring grains establish a plane which is perpendicular to the boundary surface. Contrarily, in the TGB, this plane is parallel to the boundary surface.

Tilt grain boundary structure and motion have been investigated intensively both experimentally[32,34−36,39,41,44−47] and theoretically.[29,30,35,48−50] Gido et al.[39] explored tilt grain boundary morphologies in poly(styrene-*b*-butadiene) lamellar diblock copolymers using transmission electron microscopy (TEM). Matsen examined symmetric tilt grain boundaries in the diblock copolymer lamellar phase by the application of self-consistent-field theory (SCFT).[48] The method introduced by Matsen was later applied for calculation tilt boundary structure and properties by Schick and co-workers.[49,50] The motion of a tilt boundary in a poly(styrene-*b*-ethylene propylene) lamellar diblock copolymer was studied in the presence of an external shear field by Winey and co-workers.[34−36] They characterized boundary morphologies using TEM and small-angle X-ray scattering (SAXS) measurements. In their experiments it was observed that a tilt grain boundary moves via a mechanism of lamellar rotation if the shear strain exceeds a certain critical value. The motion of a tilt grain boundary under oscillatory shear flow was examined by Viñals and co-workers.[29,30] Their mesoscopic model utilizes an expansion of the free energy in an order parameter, which evolution obeys a time-dependent Ginzburg−Landau equation. They reported on the detailed mechanisms of tilt grain boundary motion which is propelled by the shear.

The structure of TGBs in lamellar diblock copolymer melts has been analyzed by Gido et al.[39,40] Two types of TGBs have been observed: the helicoid section boundary at low twist angles and the doubly periodic morphology approximating Scherk's first surface.[51] Scherk's first surface has been proposed as a model for high angle twist boundary in lamellar systems by Thomas et al.[52] The TGB has been also experimentally investigated by Nishikawa et al.[41] Both Gido et al.[39] and Nishikawa et al.[41] compared their experimental two-dimensional (2D) TEM images with 3D computer simulations using suitable mathematical models with no physical interactions involved. A few theoretical studies have been devoted to TGB structure.[53,54] Duque and Schick applied the SCFT of Matsen to TGBs of lamellar block copolymer melts.[53] They treated the TGB as an equilibrium block copolymer morphology. They proposed the linear stack of dislocations to be a better representation of the TGB than Scherk's first surface. Kamien and Lubensky performed phenomenological calculations to show that the TGB is not given by either the linear stack of dislocations or Scherk's first surface and that there is no essential difference between the two descriptions.[54] To our knowledge, there are no studies on the motion of a TGB in either an external electric field or shear.

The aim of the present study is to investigate 3D structure and motion of TGBs in lamellae diblock copolymer melts in an external electric field. The block copolymer morphology evolution is examined in the framework of a mean-field dynamic density functional theory (DDFT).[55,56] Since the grain boundary structures are metastable defects, but not a thermodynamic phase, the study of TGB motion requires dynamical consideration. To this end, the SCFT is not applicable for investigation of grain boundary motion. By construction DDFT generates metastable morphologies and gives a possibility to track the structure and dynamics of a single defect. An advantage of DDFT is that the method is based on a molecular description of polymer liquids, without any bias with respect to the morphology formation. The DDFT works well in three dimensions and allows for the description of a specific complex polymer liquid. Yet only mathematical software with no molecular details has been used to mimic 3D images of grain boundaries.[39,41] Our study gives the 3D morphology of a TGB and clarifies the mechanism of a TGB motion.

II. Theoretical Framework and Numerical Evaluation

The block copolymer melt is modeled as a compressible system of Gaussian chain molecules in a mean-field environment. The free energy functional for a block copolymer melt has the form[25,26]

$$F[\rho] = -\beta^{-1} \ln\left(\frac{\Phi^n}{n!}\right) - \sum_I \int_V U_I(\mathbf{r})\, \rho_I(\mathbf{r})\, \mathrm{d}\mathbf{r} + F^{\mathrm{nid}}[\rho] + F_{\mathrm{el}}[\rho] \quad (1)$$

where $\beta^{-1} = k_B T$ and Φ is the intramolecular partition function for the ideal Gaussian chain in the external potential U_I. We consider a diblock copolymer melt of the volume V which contains n diblock copolymer Gaussian chains, each of length $N = N_A + N_B$. In such a system there are two concentration fields $\rho_A(\mathbf{r})$ and $\rho_B(\mathbf{r})$, two external potentials $U_A(\mathbf{r})$ and $U_B(\mathbf{r})$ conjugated to the concentration fields ρ_A and ρ_B, respectively. The nonideal free energy F^{nid} describes the mean-field interaction between chemically different blocks and the interaction of a block copolymer with surfaces.[55−59] The system is subjected to an external electric field $\mathbf{E}_0$. The electrostatic contribution F_{el} to the free energy accounts for the interaction between the melt and the electric field.[25,26]

The time evolution of the concentration fields $\rho_I(\mathbf{r})$ in the presence of an external electric field $\mathbf{E}_0$ applied parallel to the z-axis of laboratory coordinate system can be described by a stochastic diffusion equation[25,26]

$$\frac{\partial \rho_I(\mathbf{r})}{\partial t} = M\nabla^2 \mu_I^0(\mathbf{r}) + M\beta^{-1}\nu B \nabla_z^{\,2} \rho_I(\mathbf{r}) + \eta_I(\mathbf{r},t) \quad (2)$$

Here, μ_I^0 is the intrinsic chemical potential of the system in the absence of the applied electric field, η_I is the thermal noise, M is the mobility coefficient, and ν is the average volume of the statistical unit (the same for all beads). The dimensionless electric field parameter B can be expressed as[25,26]

$$B = \frac{1}{\pi}\beta\nu \frac{(\epsilon_A - \epsilon_B)^2}{\epsilon_A + \epsilon_B} {E_0}^2 \quad (3)$$

where ϵ_A and ϵ_B are the dielectric constants of two pure copolymer components A and B, respectively.

The equation of motion (2) was numerically integrated by a Crank−Nicolson scheme. We consider 3D systems of a model symmetric diblock copolymer melt A_8B_8 exhibiting lamellar morphology. The cubic grid is $32 \times 32 \times 32$. The dimensionless parameters have been chosen as (see details in refs 25, 55, and 56): the dimensionless time step $\Delta\tau \equiv \beta^{-1}\nu M h^{-2}\Delta t = 0.5$ (h is

the mesh size of the physical grid), the grid parameter $d \equiv ah^{-1} = 1.1543$ (a is the Gaussian chain bond length[56]), the noise scaling parameter $\Omega \equiv \nu^{-1}h^3 = 100$, the compressibility parameter $\kappa_H' \equiv \beta\kappa_H\nu = 30$, and the electric field parameter $BN = 0.32$ ($E_0 \sim 10^7$ V/m). The interaction parameters between different blocks of a copolymer melt have been chosen to be $\beta\epsilon^0_{AA}/\nu = \beta\epsilon^0_{BB}/\nu = 0.0$ and $\beta\epsilon^0_{AB}/\nu = 3.0$, so that $\chi N = 19$ (χ is the Flory–Huggins interaction parameter). The interaction parameters between blocks and the bounding electrode surfaces are $\beta\epsilon^0_{BS}/\nu = 0.0$ and $\beta\epsilon^0_{AS}/\nu = 0.7$ if not indicated otherwise, corresponding to the adsorption energy $0.28k_BT$ per statistical unit. It means that the electrode surfaces are selective for copolymer blocks: the surfaces are indifferent to B blocks and repel A blocks. The situation of two identical parallel surfaces is considered.

In the direction perpendicular to the electrode surfaces we use rigid-wall boundary conditions, fulfilled by allowing no flux through the surfaces:[26,57]

$$\nabla\mu_I \cdot \mathbf{n}_S = 0 \tag{4}$$

where $\mathbf{n}_S$ is the normal to the surfaces, directed in this particular study along the z-axis of laboratory coordinate system. The rigid-wall boundary conditions in this direction are also employed for the noise η_I. In all other directions periodic boundary conditions are applied. As initial conditions, we consider a homogeneous distribution of all components, $\rho_I(\mathbf{r}) = \rho^0_I$.

We quenched the homogeneous melt, and applied the electric field and surface interactions simultaneously. The surfaces and the electric field compete with each other and tend to align the lamellar microstructure in perpendicular directions. The applied electric field aligns lamellar planes parallel to the electric field direction, whereas the surface field orients lamellae parallel to the surfaces, i.e., perpendicular to the electric field. Depending on the relative strength of the two competing fields, the system exhibits parallel or perpendicular orientation. In the present study, polymer–surface interaction parameters have been chosen to be weak enough, so that the final lamellae structure is always parallel to the electric field.

III. Results and Discussion

In Figure 1 we present the time evolution of lamellae pattern and the z-projection of the 3D structure factor $S(\mathbf{k}) = \langle|\rho_A(\mathbf{k})|^2\rangle$ in a film of a symmetric diblock copolymer melt in the presence of an external electric field. Figure 1a shows a not yet phase-separated microstructure at a very early time. One can clearly observe that near the surface a one layer starts to form. This layer parallel to the surface is highly deformed, with many holes, because of a relatively small interaction with surfaces. The presence of two layers parallel to the surfaces gives two reflections into a scattering pattern, which are projected to one sharp central peak in the k_xk_y plane. The regions inside a film, quite far from the electrode surfaces, contain still growing lamellae locally correlated but globally randomly oriented somewhat similar to phase separation in bulk.[25] The corresponding scattering function shown in the k_xk_y plane is an isotropic ring. The influence of an electric field is not visible at this level of phase separation. The stage of complete prevalence of electric field alignment over surface alignment is shown in Figure 1b. The

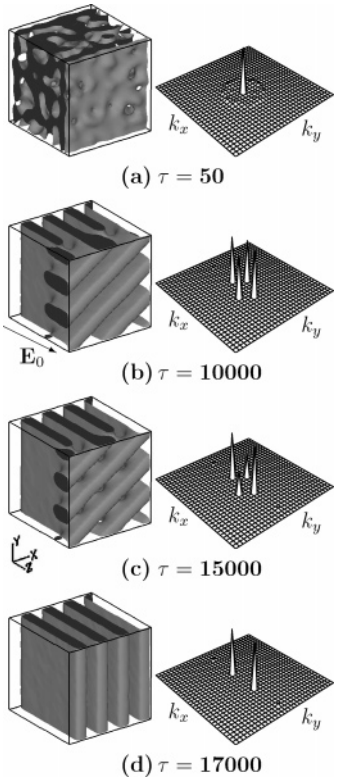

Figure 1. Isosurface representation of a symmetric diblock copolymer melt for $\nu\rho_A = 0.5$ and the z projection of the 3D structure factor $S(\mathbf{k})$ at different dimensionless times τ. The motion of a twist grain boundary of two-grain lamellar morphology in an external electric field is shown. As time evolves, one grain is invaded by lamellae of the other grain, until a uniform lamellar configuration occupies the whole system.

lamellae parallel to the surfaces are destroyed by electric field. This corresponds to complete annihilation of the central peak in the z-projection of the 3D structure factor. A structure shown in Figure 1b consists of two coexisting lamellae clusters (grains) with lamellae being straight and parallel to the electric field, but oriented differently in the xy plane perpendicular to the electric field. An accompanied scattering pattern demonstrates two pairs of sharp Bragg peaks related to these grains. From Figure 1b one can see that the normals perpendicular to the lamellae of the two grains define a plane which is parallel to the plane of the boundary. Thus, the observed grain boundary is a TGB. The presence in a system of two lamellae grains twisted with respect to each other is not likely due to additional interfacial interactions between grains. The grain boundary region, which can be treated as a surface, the so-called intermaterial dividing surface (IMDS), costs an energy to the system. This surface is a defect in the microstructure, and it is thermodynamically unstable. There are several possibilities to remove a defect and to align a microstructure. The whole lamellae grain can start turning to coincide the orientation of a neighboring grain. This rigid-body-like mechanism of domain reorientation involves a huge free energy barrier and is therefore very unlikely. Another mechanism, that of selective disordering, consistent with a melting of lamellae in unfavorable orientations and re-formation of lamellae in preferable orientations, is also very unlikely on the basis of energetic arguments.[6–8] The most convenient mechanism of mesophase reorientation in thin films conforms to defect movement, which we already observed for bulk

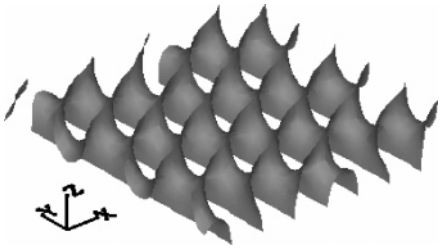

Figure 2. Enlarged part of two-grain morphology shown in Figure 1b containing the twist grain boundary (the z position ranges between $z = 17$ and $z = 23$). The region exhibits a doubly periodic array of saddle surfaces resembling Scherk's first surface twist grain boundary morphology.

systems.[25] In regard to the situation monitored here, the IMDS moves in the direction of an electric field, as is shown in Figure 1b,c, until only one set of lamellae survives (Figure 1d). The selection of survived and annihilated lamellae is determined by the fitting of lamellar period into the box and will be discussed later. While moving a grain boundary the volume fraction of one cluster increases with decreasing of another one. The corresponding scattering peaks change their intensity. From Figure 1b,c one can see the evident decrease of intensity of two peaks related to the grain containing inclined with respect to box planes lamellae. Such changes in a structure factor can be experimentally observed with the help of SAXS or small-angle neutron scattering (SANS) measurements. The final morphology in Figure 1d consists of perfect lamellae parallel to the electric field. A z projection of 3D structure factor exhibits two strong first-order Bragg peaks even with visible peaks of second order and confirms a perfect lamellae alignment in the applied electric field direction.

A peculiar effect is the grain boundary morphology between the two lamellae grains (Figure 1b,c). In Figure 2 the cropped morphology of Figure 1b containing the grain boundary region (the z-position ranges between $z = 17$ and $z = 23$) at time $\tau = 10\,000$ is shown at a different view angle. As can be seen from Figure 2, this region consists of a doubly periodic array of saddle surfaces, similar to Scherk's first surface twist boundary morphology.[51] In our case, this grain boundary structure approximates a minimal surface with respect to minimization of the total free energy of a block copolymer sample in an electric field but is not exactly Scherk's minimal surface. Minimal surfaces are solutions to mathematical problems involving only area minimization. Physical solutions obtained by minimization of the free energy functional, which contains the contribution of chain conformational energies, cannot be exactly minimal surfaces in many cases.[60−62] Also, the electrostatic contribution to the free energy can also lead to the deviation of the block copolymer grain boundary interface from the minimal surface. The role of the electric field will be addressed later.

The TGB morphology shown in Figures 1b and 2 can be better seen in Figure 3, in which the 2D morphology scans through the neighboring xy planes are performed. From Figure 3 one can observe all intermediate lamellar morphologies from one grain of straight lamellae to another. These doubly periodic lamellae morphologies, obtained by cutting the microstructure at different positions of a grain boundary interface, look differently and can help to indicate the presence of saddle surfaces in a microstructure for TEM or scanning electron microscopy (SEM) measurements.

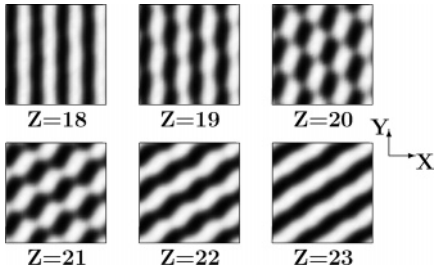

Figure 3. Morphology scans through the Scherk twist grain boundary in the same ranges as shown in Figure 2. The morphologies shown are xy orthoslices of two-grain lamellar structure from Figure 1b at different z positions. In these gray scale plots, the darker shading corresponds to larger density of A blocks with linear gray scale of the dimensionless density $\nu\rho_A$ from 0.0 black to 1.0 white.

Our simulations give a possibility to trace the dynamics of every single defect in a microstructure and to directly observe grain boundary motion and structure. An important result of the simulations is that a TGB interface remains intact, and a grain boundary structure does not change its profile during TGB motion. This result supports a hypothesis of Hu et al.,[63] based on their very recent grain growth experiments, about the mechanism of TGB motion. The hypothesis suggests that, in contrast with tilt grain boundaries, TGBs move via a mechanism in which the TGB interfaces are unbroken; i.e., only diffusion parallel to the interfaces is necessary. Contrary, for tilt grain boundaries some interfacial breaking and re-forming are required, i.e., diffusion of chains perpendicular to the lamellar planes.

Now, we will clarify a driving force for moving of a boundary between lamellae grains shown in Figure 1b,c. From the evolution of the defect structures, we calculated the speed of boundary movement which remains constant during the re-formation of lamellar microstructure except in the initial stage of creation of this grain boundary and that of its disappearance. The transversal motion of the defect structure of one cell in the system takes more than 10^3 time units while the boundary passes the distance approximately equal to 10 grid points. As the radius of gyration R_g of the polymers is about 4 grid points and one unit of time is smaller than the polymer relaxation time, this means that the polymer is in quasi-equilibrium with respect to the defect structure. The anisotropic diffusion processes at the IMDS propel the motion of the surface. A relocation of the surface is not affected by an electric field. At least, the influence of an electric field on boundary movement is too small to be observed. The driving force of grain boundary movement at this very late stage of almost completely aligned lamellae in the direction of an applied field is a thermodynamic force $\nabla\mu_I^0$ related to part F_0 of the total free energy F of the sample without the electrostatic contribution F_{el}.

The changes in a free energy F_0 can be observed from Figure 4. Figure 4 shows that while moving of the IMDS there is almost no change (except thermal fluctuations) in the free energy of the system. It is consistent with the fact that the TGB morphology is preserved in the course of the grain boundary movement. After the annihilation of the grain boundary nearly at $\tau = 16\,750$, the free energy F_0 drops down and reaches the lowest level, as shown in the inset of Figure 4. Thus, the small energetic difference between the lamellar structures with and without a grain boundary is the driving force for the annihilation of grain boundaries.

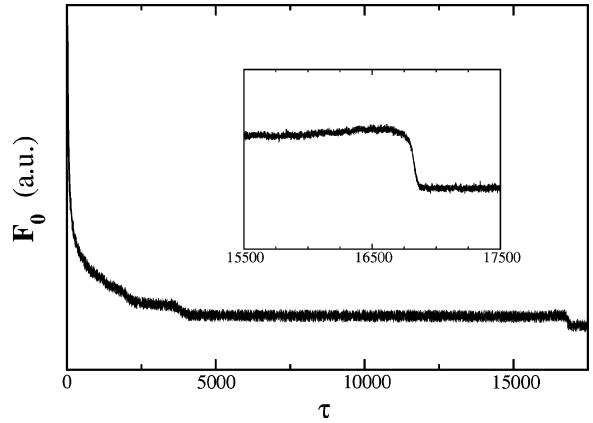

Figure 4. Part F_0 of the total free energy of the diblock copolymer without the electrostatic contribution as a function of time τ. The graph shows changes in the free energy during twist grain boundary motion.

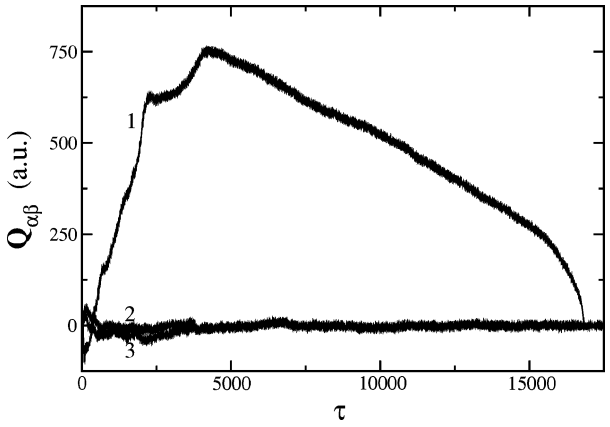

Figure 5. Time evolution of stresses in the morphology $Q_{\alpha\beta}$ due to domains (the contributions due to changes in chain conformations are not included): Q_{xy} (curve 1), Q_{xz} (curve 2), and Q_{yz} (curve 3).

The spatial anisotropy of a block copolymer microstructure can be displayed with the help of the volume-averaged factors $Q_{\alpha\beta} = \langle \nabla_\alpha \rho_A \nabla_\beta \rho_A \rangle$ ($\alpha, \beta = x, y, z$; $\alpha \neq \beta$), which are related to the stress tensor due to domains.[64−66] For specificity, we have taken the concentration of A component. These anisotropy factors $Q_{\alpha\beta}$ represent the domain contribution to the stress tensor arising from the composition inhomogeneities; they do not represent the contribution due to changes in chain conformations. The time evolution of stresses in the morphology $Q_{\alpha\beta}$ due to domains is shown in Figure 5. The sharp increase of Q_{xz} (curve 2 in Figure 5) and Q_{yz} (curve 3) as well as decrease of Q_{xy} (curve 1) until $\tau \simeq 100$ corresponds to the formation of sharp lamellae boundaries. Further reorientation of lamellar under the influence of an electric field causes a gradual decline of Q_{xz} and Q_{yz} with some deviations. The xy component of the stress tensor demonstrates more interesting behavior. The intense increase of Q_{xy} is caused by growing of lamellar grains parallel to the electric field direction, but twisted with respect to each other. Such a twist in xy plane costs a large stress compared with other components of the stress tensor. While later disappearance of one of the grains from $\tau \simeq 4250$ until the formation of final structure at $\tau \simeq 17\,000$, from Figure 5 it follows that the anisotropy factor Q_{xy} decreases. The final morphology of perfect lamellae gives no contributions to the stress tensor due to domain deformations,

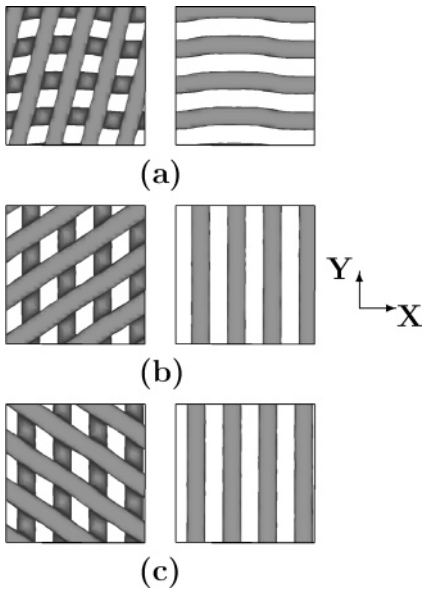

Figure 6. Intermediate structures of two coexisting grains of lamellae parallel to the electric field twisted in different angles with respect to one another and the final uniform lamellar morphology for the surface related interaction parameters (a) $\beta\epsilon^0_{AS}/\nu = 0.5$, (b) 0.7, and (c) 0.8. A view along the direction of the applied electric field is shown.

consistent with the zero value reached by all anisotropy factors $Q_{\alpha\beta}$.

We also performed simulations with different surface related interaction parameter $\beta\epsilon^0_{AS}/\nu$, which led to the same final structures of perfect lamellae shown in Figure 6. Figure 6 shows an intermediate structure of two coexisting lamellar grains of lamellae parallel to the electric field and a final morphology in the case of interaction parameters with the surfaces $\beta\epsilon^0_{AS}/\nu = 0.5$ (Figure 6a), 0.7 (Figure 6b), and 0.8 (Figure 6c). In Figure 6 one sees projections in the z direction of the external electric field. From Figure 6 it can be concluded that a film of a block copolymer material exhibits uniaxial symmetry with respect to the applied electric field direction. The lamellae planes aligned by an electric field contain the electric field vector, but they can be oriented differently perpendicular to the electric field plane (xy). All these states have the same energy. This type of rotational symmetry is clearly observed from the final lamellar morphologies, shown in Figure 6, where lamellae can form in principle different angles with x and y axes. In general, the angle between the grains depends on a pathway of mesophase formation. Particularly, the distribution of defects such as holes and necks and their development in time affects the orientation of the grains. In simulations we observed only final morphologies with lamellae parallel to the x or y axis (to the side box planes) due to periodic boundary conditions applied in x and y directions and due to the best fitting of lamellar period into the box size in x and y directions. Intermediate structures with two lamellae grains confirm the best fitting of lamellar period in the case where lamellae are parallel to one of the side box planes. In these directions the integer number of lamellae matches the box size. In such a case lamellae layers are unstrained. From Figure 6 one can see that inclined lamellae of two-grain morphology do not fit well into the box in all slanted directions. In the slanted directions a noninteger number of lamellae fits into the box. As a result, large stresses are induced in

the system (see Figure 5). The above arguments of lamellae fitting into the box can be considered as those which model a real multigrain structure. In an actual block copolymer sample, a lamellar grain is confined within other grains and fits into some directions better than into others. Many of the grains will be oriented in directions for which the fitting is not the best, resulting in large stresses.

From real-space images of a TGB morphology shown in Figures 1−3 and 6 we have found the dimensionless width W/L of the Scherk grain boundary. The TGB width W is about the lamellar period L for the investigated degree of phase segregation, $W/L \simeq 1$. This result is in perfect agreement with experiments of Gido and Thomas.[40] The obtained by TEM micrographs of Scherk surfaces having different twist angle displayed grain boundary width of about a lamellar period. This result implies that the TGB interface essentially is built from one layer of block copolymer chains, so the distance a grain boundary penetrates into two lamellar grains is about $2R_g$. Also, we observed that the twist bandwidth is constant with TGB movement.

We have used an external electric field to create TGBs in block copolymer melts and to investigate the TGB movement. The electric field suppresses tilt grain boundaries and facilitates the creation of TGBs due to symmetry reasons. Uniaxial symmetry of a system with respect to the applied electric field direction results in appearance of lamellae grains with lamellae parallel to the electric field, which are separated by a grain boundary oriented perpendicular to the field. In such a case, the TGB has no tilt component. This makes the situation less complex for investigation of diffusion process at the grain boundary interface. The study of the diffusivity of the block copolymer molecules can give more information about chain dynamics in microstructured block copolymers.[67−72] Since the TGB moves in the direction of an electric field, only diffusion parallel to the grain boundary interface is required.

The investigation of the dynamics of a TGB is of interest itself. To our knowledge, only static theories of TGBs in block copolymers have been developed.[39,40,53,54] The dynamics of a grain boundary have been studied only in the case of tilt grain boundaries subjected to a shear flow.[29,30,34−36] The shear flow has different symmetry than an electric field due to the presence of two principal directions: the shear velocity and the shear velocity gradient direction. As a result, it is difficult to create a pure TGB in a shear flow. A TGB in a shear flow most likely contains a significant tilt component.

The difference in symmetry of shear and electric field leads to different mechanisms of grain boundary motion. Viñals and co-workers[29,30] have found that the grain boundary moves by the action of the shear. The results of our simulations show that the movement of the TGB is not affected by the electric field. The reason is in different character of the defect annihilation mechanism, which we already observed before.[25] In contrast with microstructured fluids in an electric field, in the sheared systems, defects are convected by the flow field.[27,28,33] As a result, we also did not observe the mechanism of grain boundary rotation, which was monitored in experiments of Qiao et al. in the case of a tilt boundary.[34−36] Because of difficulties in creation of a pure TGB in a shear flow, TGB motion under shear flow has not been investigated yet. It would be interesting to compare a TGB kinetics in shear and in an electric field. We expect that the mechanisms of TGB motion under shear will be different from those in an electric field. Another attractive aspect of a grain boundary kinetics is the mechanism of TGB motion under the action of a temperature gradient, i.e., during heat treatment (annealing) of a sample. Despite the difference in nature of a temperature gradient and electric field, in the case of alignment of a lamellar morphology during heat treatment one might expect the same driving force for the annihilation of grain boundaries due to the energetic difference between the lamellar microstructure with and without a grain boundary. A comparative analysis of the effect of temperature gradient, shear, and electric field on TGB motion should be a topic of further investigation.

Our computer simulations allow us to monitor 3D block copolymer structures as well as 2D morphology scans through the structures. In particular, the simulations can give insight into a 3D grain boundary structure. Because of lack of 3D imaging techniques, little is known about the structures of these defects. There is a limited number of experimental methods to reconstruct a 3D morphology from a series of 2D images, using laser scanning confocal microscopy (LSCM)[60−62,73,74] or scanning probe microscopy (SPM).[75] Therefore, our theoretical approach together with the method of inverse mapping for 3D structure reconstruction from a 2D morphology recently developed in our group[76] can serve as an additional powerful tool for studying 3D grain boundary structures, which complements experiments on 3D real-space volume imaging. Our computer simulations of 3D images of block copolymer grain boundaries are one step further toward the hybrid modeling in combinatorial polymer research.[77]

IV. Conclusions

We have studied 3D structure and motion of twist grain boundaries in lamella forming diblock copolymer melts in the presence of an electric field. The method used is a mean-field dynamic density functional theory with electrostatic interactions incorporated into the model. The observed twist grain boundary structure consists of a doubly periodic array of saddle surfaces, similar to Scherk's first surface, which was noticed in many experiments.[39−41,52] We have found that the twist grain boundary interface remains unbroken and the grain boundary structure keeps its profile constant with twist grain boundary motion. This supports a hypothesis of Hu et al.,[63] based on their grain growth experiments, which suggests that twist grain boundaries move via a mechanism in which the twist grain boundary interfaces are intact; i.e., only diffusion parallel to the interfaces is required. Since a grain boundary can be considered as a defect in the microstructure, twist grain boundary motion is a specific case of defect movement mechanism of mesophase reorientation. We did not observe another mechanisms of domain reorientation, such as selective disordering and rigid-body-like mechanism of domain rotation, in accord with earlier predictions.[6−8,25,26]

The results of our simulations show that the movement of a twist grain boundary is not affected by the electric field. At least, the influence of an electric field on grain boundary movement is too small to be observed. This contrasts with grain boundary motion under shear flow. For tilt grain boundaries it was found that the grain boundary moves by the action of the shear.[29,30,34−36] Such a distinction in behavior is caused by the difference

in symmetry of shear and electric field. In contrast with microscopically phase-separated block copolymers in an electric field, in the sheared systems, defects of all types are convected by the flow field. Because of difference in defect movement mechanisms, we expect that a twist grain boundary movement under shear flow will be also driven by the shear, changing the picture of a twist grain boundary movement observed here.

An electric field is a perfect candidate for investigation of twist grain boundaries and their dynamics. Uniaxial symmetry of a system with respect to the applied electric field results in suppression of tilt grain boundaries and creation of twist grain boundaries between grains with lamellae parallel to the electric field, but oriented differently in perpendicular to the electric field direction.

The width of a twist grain boundary is found to be about the lamellar period for all the observed twist angles, in agreement with experiments of Gido and Thomas.[40] This validates the fact that the twist grain boundary interface essentially is built from one layer of diblock copolymer chains. The twist bandwidth stays constant while twist grain boundary motion.

We have monitored the time evolution of the domain contribution to the stress tensor arising from the composition inhomogeneities (the contribution due to changes in chain conformations is not considered). Lamellae grains twisted with respect to each other lead to a large stress tensor component due to domains in the twist grain boundary plain. The results suggest that in a real multigrain microstructure the existence of twisted lamellae grains, which are confined within other grains and might fit not in the best way, results in large stresses in the system.

Because of lack of experimental techniques on 3D real-space volume imaging and technical complications in performing such experiments, little is known about the grain boundary structures. Our theoretical approach can provide information about 3D grain boundary structures and their dynamics.

References and Notes

(1) Hamley, I. W. *The Physics of Block Copolymers*; Oxford University Press: New York, 1998.
(2) Bates, F. S.; Fredrickson, G. H. *Phys. Today* **1999**, *52*, 32.
(3) Fredrickson, G. H.; Bates, F. S. *Annu. Rev. Mater. Sci.* **1996**, *26*, 501.
(4) Fink, Y.; Winn, J. N.; Fan, S.; Chen, C.; Michel, J. D.; Jonnapoulos, J. D.; Thomas, E. L. *Science **1998**, 282*, 1679.
(5) Park, M.; Harrison, C.; Chaikin, P. M.; Register, R. A.; Adamson, D. H. *Science* **1998**, *276*, 1401.
(6) Amundson, K.; Helfand, E.; Davis, D. D.; Quan, X.; Patel, S. S.; Smith, S. D. *Macromolecules* **1991**, *24*, 6546.
(7) Amundson, K.; Helfand, E.; Quan, X.; Smith, S. D. *Macromolecules* **1993**, *26*, 2698.
(8) Amundson, K.; Helfand, E.; Quan, X.; Hudson, S. D.; Smith, S. D. *Macromolecules* **1994**, *27*, 6559.
(9) Onuki, A.; Fukuda, J. *Macromolecules* **1995**, *28*, 8788.
(10) Gurovich, E. *Phys. Rev. Lett.* **1995**, *74*, 482.
(11) Morkved, T. L.; Lu, M.; Urbas, A. M.; Ehrichs, E. E.; Jaeger, H. M.; Mansky, P.; Russell, T. P. *Science* **1996**, *273*, 931.
(12) Mansky, P.; DeRouchey, J.; Russell, T. P.; Mays, J.; Pitsikalis, M.; Morkved, T.; Jaeger, H. *Macromolecules* **1998**, *31*, 4399.
(13) Thurn-Albrecht, T.; DeRouchey, J.; Russell, T. P.; Jaeger, H. M. *Macromolecules* **2000**, *33*, 3250.
(14) Thurn-Albrecht, T.; DeRouchey, J.; Russell, T. P.; Kolb, R. *Macromolecules* **2002**, *35*, 8106.
(15) DeRouchey, J.; Thurn-Albrecht, T.; Russell, T. P.; Kolb, R. *Macromolecules* **2004**, *37*, 2538.
(16) Xu, T.; Hawker, C. J.; Russell, T. P. *Macromolecules* **2003**, *36*, 6178.
(17) Xu, T.; Goldbach, J. T.; Russell, T. P. *Macromolecules* **2003**, *36*, 7296.
(18) Xu, T.; Zhu, Y.; Gido, S. P.; Russell, T. P. *Macromolecules* **2004**, *37*, 2625.
(19) Xu, T.; Goldbach, J. T.; Leiston-Belanger, J.; Russell, T. P. *Colloid Polym. Sci.* **2004**, *282*, 927.
(20) Böker, A.; Knoll, A.; Elbs, H.; Abetz, V.; Müller, A. H. E.; Krausch, G. *Macromolecules* **2002**, *35*, 1319.
(21) Pereira, G. G.; Williams, D. R. M. *Macromolecules* **1999**, *32*, 8115.
(22) Ashok, B.; Muthukumar, M.; Russell, T. P. *J. Chem. Phys.* **2001**, *115*, 1559.
(23) Tsori, Y.; Andelman, D. *Macromolecules* **2002**, *35*, 5161.
(24) Feng, J.; Ruckenstein, E. *J. Chem. Phys.* **2004**, *121*, 1609.
(25) Kyrylyuk, A. V.; Zvelindovsky, A. V.; Sevink, G. J. A.; Fraaije, G. J. E. M. *Macromolecules* **2002**, *35*, 1473.
(26) Kyrylyuk, A. V.; Sevink, G. J. A.; Zvelindovsky, A. V.; Fraaije, G. J. E. M. *Macromol. Theory Simul.* **2003**, *12*, 508.
(27) Chen, Z. R.; Kornfield, J. A. *Polymer* **1998**, *39*, 4679.
(28) Zvelindovsky, A. V.; Sevink, G. J. A.; van Vlimmeren, B. A. C.; Maurits, N. M.; Fraaije, G. J. E. M. *Phys. Rev. E* **1998**, *57*, R4879.
(29) Huang, Z. F.; Drolet, F.; Viñals, J. *Macromolecules* **2003**, *36*, 9622.
(30) Huang, Z. F.; Viñals, J. *Phys. Rev. E* **2004**, *69*, 041504.
(31) Balsara, N. P.; Hammouda, B. *Phys. Rev. Lett.* **1994**, *72*, 360.
(32) Wang, H.; Newstein, M. C.; Chang, M. Y.; Balsara, N. P.; Garetz, B. A. *Macromolecules* **2000**, *33*, 3719.
(33) Ren, S. R.; Hamley, I. W.; Teixeira, P. I. C.; Olmsted, P. D. *Phys. Rev. E* **2001**, *63*, 041503.
(34) Qiao, L.; Winey, K. I. *Macromolecules* **2000**, *33*, 851.
(35) Qiao, L.; Winey, K. I.; Morse, D. C. *Macromolecules* **2001**, *34*, 7858.
(36) Qiao, L.; Ryan, A. J.; Winey, K. I. *Macromolecules* **2002**, *35*, 3596.
(37) Hashimoto, T.; Bodycomb, J.; Funaki, Y.; Kimishima, K. *Macromolecules* **1999**, *32*, 952.
(38) Bodycomb, J.; Funaki, Y.; Kimishima, K.; Hashimoto, T. *Macromolecules* **1999**, *32*, 2075.
(39) Gido, S. P.; Gunther, J.; Thomas, E. L.; Hoffman, D. *Macromolecules* **1993**, *26*, 4506.
(40) Gido, S. P.; Thomas, E. L. *Macromolecules* **1994**, *27*, 849.
(41) Nishikawa, Y.; Kawada, H.; Hasegawa, H.; Hashimoto, T. *Acta Polym.* **1993**, *44*, 247.
(42) Hirth, J. P.; Lothe, J. *Theory of Dislocations*; John Wiley and Sons: New York, 1975.
(43) Kamien, R. D. *Rev. Mod. Phys.* **2002**, *74*, 953.
(44) Burgaz, E.; Gido, S. P. *Macromolecules* **2000**, *33*, 8739.
(45) Cohen, Y.; Albalak, R. J.; Benita, D. J.; Capel, M. S.; Thomas, E. L.; *Macromolecules* **2000**, *33*, 6502.
(46) Yang, L.; Hong, S.; Gido, S. P.; Velis, G.; Hadjichristidis, N. *Macromolecules* **2001**, *34*, 9069.
(47) Chang, M. Y.; Abuzaina, F. M.; Kim, W. G.; Gupton, J. P.; Garetz, B. A.; Newstein, M. C.; Balsara, N. P.; Yang, L.; Gido, S. P.; Cohen, R. E.; Boontongkong, Y.; Bellare, A. *Macromolecules* **2002**, *35*, 4437.
(48) Matsen, M. W. *J. Chem. Phys.* **1997**, *107*, 8110.
(49) Netz, R. R.; Andelman, D.; Schick, M. *Phys. Rev. Lett.* **1997**, *79*, 1058.
(50) Duque, D.; Katsov, K.; Schick, M. *J. Chem. Phys.* **2002**, *117*, 10315.
(51) Scherk, H. F. *Reine Angew. Mater.* **1835**, *13*, 185.
(52) Thomas, E. L.; Anderson, D. M.; Henkee, C. S.; Hoffman, D. *Nature (London)* **1988**, *334*, 598.
(53) Duque, D.; Schick, M. *J. Chem. Phys.* **2000**, *113*, 55255.
(54) Kamien, R. D.; Lubensky, T. C. *Phys. Rev. Lett.* **1999**, *82*, 2892.
(55) Fraaije, J. G. E. M. *J. Chem. Phys.* **1993**, *99*, 9202.
(56) Fraaije, J. G. E. M.; van Vlimmeren, B. A. C.; Maurits, N. M.; Postma, M.; Evers, O. A.; Hoffmann, C.; Altevogt, P.; Goldbeck-Wood, G. *J. Chem. Phys.* **1997**, *106*, 4260.
(57) Sevink, G. J. A.; Zvelindovsky, A. V.; van Vlimmeren, B. A. C.; Maurits, N. M.; Fraaije, J. G. E. M. *J. Chem. Phys.* **1999**, *110*, 2250.
(58) Kyrylyuk, A. V.; Fraaije, J. G. E. M. *J. Chem. Phys.* **2004**, *121*, 2806.
(59) Kyrylyuk, A. V.; Fraaije, J. G. E. M. *J. Chem. Phys.* **2004**, *121*, 9166.
(60) Jinnai, H.; Koga, T.; Nishikawa, Y.; Hashimoto, T.; Hyde, S. T. *Phys. Rev. Lett.* **1997**, *78*, 2248.
(61) Jinnai, H.; Nishikawa, Y.; Hashimoto, T. *Phys. Rev. E* **1999**, *59*, R2554.
(62) Jinnai, H.; Nishikawa, Y.; Spontak, R. J.; Smith, S. D.; Agard, D. A.; Hashimoto, T. *Phys. Rev. Lett.* **2000**, *84*, 518.

(63) Hu, X.; Zhu, Y.; Gido, S. P.; Russell, T. P.; Iatrou, H.; Hadjichristidis, N.; Abuzaina, F. M.; Garetz, B. A. *Faraday Discuss.* **2005**, *128*, 103.
(64) Onuki, A. *Phys. Rev. A* **1987**, *35*, 5149.
(65) Onuki, A. *J. Phys.: Condens. Matter* **1997**, *9*, 6119.
(66) Ohta, T.; Nozaki, H.; Doi, M. *Phys. Lett. A* **1990**, *145*, 304.
(67) Dalvi, M. C.; Lodge, T. P. *Macromolecules* **1993**, *26*, 859.
(68) Dalvi, M. C.; Eastman, C. E.; Lodge, T. P. *Phys. Rev. Lett.* **1993**, *71*, 2591.
(69) Hamersky, M. W.; Tirrell, M.; Lodge, T. P. *Macromolecules* **1981**, *14*, 6974.
(70) Lodge, T. P.; Dalvi, M. C. *Phys. Rev. Lett.* **1995**, *75*, 657.
(71) Ehlich, D.; Takenaka, M.; Okamoto, S.; Hashimoto, T. *Macromolecules* **1993**, *26*, 189.
(72) Ehlich, D.; Takenaka, M.; Hashimoto, T. *Macromolecules* **1993**, *26*, 492.
(73) Verhoogt, H.; van Dam, J.; Posthuma de Boer, A.; Draaijer, A.; Houpt, P. M. *Polymer* **1993**, *34*, 1325.
(74) Jinnai, H.; Nishikawa, Y.; Koga, T.; Hashimoto, T. *Macromolecules* **1995**, *28*, 4782.
(75) Magerle, R. *Phys. Rev. Lett.* **2000**, *85*, 2749.
(76) Lyakhova, K. S.; Zvelindovsky, A. V.; Sevink, G. J. A.; Fraaije, J. G. E. M. *J. Chem. Phys.* **2003**, *118*, 8456.
(77) Kyrylyuk, A. V.; Case, F. H.; Fraaije, J. G. E. M. *QSAR Comb. Sci.* **2005**, *24*, 131.

MA0509356